Arabian Journal for Science and Engineering
https://doi.org/10.1007/s13369-022-07294-3

RESEARCH ARTICLE-ELECTRICAL ENGINEERING

Condition Monitoring and Fault Diagnosis of Induction Motor using DWT and ANN

Srinivas chikkam[1] · **Sachin Singh**[1]

Received: 20 April 2022 / Accepted: 19 September 2022

Abstract
This paper presents an efficient approach to estimate the failures of various components in an induction motor using motor current signature analysis. Conventional sensor-based fault detection methods lead to huge manpower and require greater number of sensors. To overcome these drawbacks, current signature base fault detection is proposed. An advanced spectral analysis, namely discrete wavelet transform (DWT), is used for frequency domain analysis. This paper also presents fault severity estimation using feature extraction-based evaluation of DWT coefficients. As the DWT gives many coefficients at higher level decomposition which is essential for high resolution, fault classification and severity index become challenging. To address this issue, artificial neural network (ANN) algorithm is used after DWT decomposition. The fault severity is predicted by proposed fault indexing parameter of various features like energy, standard deviation, skewness, variance, RMS values. Conventional algorithms like support vector machine, k-nearest neighbour, local mean decomposition-singular value decomposition and extreme learning machine have given maximum of 98–99% accuracy, Whereas the proposed DWT-based ANN has given 100% accuracy with tanh function. Moreover, the testing loss with this function is also very less. Experimental results have affirmed the accuracy of proposed fault detection of various faults in induction motor of rating 3—Phase, 1. 5KW, 440 V and 50 Hz.

Keywords Fault classification · Fault estimations · Feature extraction · Discrete wavelet transform (DWT) · Artificial neural network (ANN) · Induction motor · Motor current signature analysis (MCSA)

1 Introduction

In most of the industries, induction motors are widely used due to rugged configuration, low cost, versatility, flexible in operation. As per great contributions of their, induction motors are referred as the industry workhorse. Even though the induction motors are rugged in construction and good in performance, they are subjected to various faults due to natural ageing problems along with other factors such as thermal, electrical and mechanical stresses, mechanical and electrical failures. The faults in induction motors are unavoidable, and early detection and remedial action ensure the drive system to operate in safe and avoids threaten normal manufacturing and, therefore, the substantial cost penalties. In addition, the operators are targeted to work with low maintenance cost and prevention of unscheduled downtime which causes loss of production and hence the revenue of the industries. Therefore, induction motor fault diagnosis along with condition monitoring becomes an essential research area [1]. In induction motor case, the research on fault diagnosis along with condition monitoring mainly focuses on early detection of incipient faults, with the results of unnecessary shutdown of process and sacrifice of quality and accuracy in products. The main part associated with a condition monitoring system contains the machinery, fault classifiers, signal-processing tools, condition monitoring sensors, monitoring result and machine models. Uncertainties and errors in fault classification can result in machine models and monitoring output that inspires the scientists to think of a powerful as well as dependable condition monitoring system. In the existing competitive by nature industry situation, state-based maintenance as well as efficient fault overseeing are getting much

✉ Srinivas chikkam
chsreenivas80@gmail.com

Sachin Singh
sachinsingh@nitdelhi.ac.in

[1] Electrical and Electronics Engineering, National Institute of Technology Delhi, Delhi, India

Published online: 10 October 2022

more value with regular maintenance as well as regular monitoring. Numerous scientists and designers have concentrated the focus of theirs on incipient fault detection as well as preventive maintenance recently [2]. Therefore, condition monitoring of induction motors using appropriate technique along with reliable and rugged algorithm is most necessary to prevent unexpected interlude of the industrial process. The signature analysis of motor current will acquire all these necessities and have many advantages like non-intrusive, cost-effective, etc. On the other hand, few drawbacks are there in the conventional FFT-based MCSA like as unable to deliver time–frequency relation, spectral leakage, poor resolution, etc.

Many resent researchers [3–9] have addressed these problems in MCSA-based condition monitoring of induction motors. In [3, 4], the ZFFT- and ZMUSIC-based fault detection is presented to improve resolution of current spectrum and requires a greater number of samples to process. This issue is addressed in [5] using short-time Fourier transform (STFT) but it leads to leakage of spectral components due to single and long window is used. The spectral leakage problem is addressed in [6] using Wigner–Ville distribution (WVD) but requires more complex calculations. Therefore, in [7–9] wavelet transform-based fault detection has been proposed and shown good results for fault indication. But DWT- and SWT-based fault detection processes have drawback due to high number of wavelet coefficients after decomposition of the signal into many levels based on speed and supply frequency. Therefore, fault classification algorithm is essential to classify and indicate the fault existence and its severity. In this regard, the proposed work involved in detection of various faults like bearing related, broken rotor-related using motor current signature analysis with DWT-based spectral analysis. In addition to this, the fault classification algorithm is applied by minimum values of DWT coefficients which are selected as inputs to the artificial neural network (ANN) [10–12]. A functional imitation of the brain is defined under ANN, by which the human decisions are simulated and draws conclusions, even whenever illustrated with irrelevant information that is complex noisy. In an induction motor achieving 100% accuracy for multiple fault detection, the suitability of proposed technique is demonstrated through the obtained results.

In the literature survey, many papers have proposed fault detection using motor current signature analysis. Wang et al. [4] have proposed fault detection using current signature analysis with high resolution by Zoom MUSIC algorithm but have more mathematical computations. This requires an algorithm to avoid unreliable fault diagnosis. To overcome this issue with ZMUSIC, Cocconcelli et al. [5] have proposed STFT-based current signature analysis. In this, the high-frequency components are missing due to fixed sized window for all frequencies. Konar et al. [7] have introduced wavelet decomposition in continuation time domain with variable sized window. Kompella et al. [8] and [9] have proposed discrete wavelet decomposition using DWT and SWT using Wiener filter cancellation. After the noise cancellation, SWT has shown good results compared to DWT. This is due to wide sense stationary nature of the current under no load condition of the motor. Saini et al. [17] have proposed multiresolution-based fault detection using multiwavelets and gives best results but vibration signals are used for analysis. This is costly and requires high manpower. Further Zaman et al. [18] have proposed complex continuous wavelet of power spectral density (PSD) to overcome the issues of vibrations signatures. But PSD computation is complex due to mathematical analysis. Moreover, other advanced spectral analysis, matrix pencil method (MPM) which gives good resolution, is proposed by Chahine et al. [20]. But MPM has only direct analysis of complete signal instead of decomposing into small signals. In the same way, other spectral tool Hilbert transform is proposed by Ramu et al. [21] and describes only rotor fault detection. On the other part, few researchers have introduced artificial intelligence-based algorithms for fault estimation and fault classification. But accuracy is the vital parameter in estimating the effectiveness of algorithm. Sadeghian et al. [28] have proposed wavelet packet decomposition (WPD) using ANN for broken rotor fault which gives only 98% accuracy, whereas Tian et al. (2015) [25] and Du, Wenliao et al. [27] have used ELM and SVM for fault classifier which gives 99. 25% and 82. 99% accuracy, respectively. Rauber et al. [26] have proposed bearing fault diagnosis using various feature parameters and fault classifiers like kNN, SVM and MLP which gives 98. 4%, 97. 9% and 96. 6% accuracy, respectively.

From the literature, it can be conclude that there is no unique fault detection method for both bearing and broken rotor faults along with 100% accuracy algorithm in fault classification. Therefore, in this work, fault detection using MCSA in a 3-phase induction motor is proposed. Both the faults like bearing related and broken rotor faults are tested using proposed methodology. High-resolution-based spectral analysis is carried out using DWT-based decomposition with Daubechies's mother wavelet of order 44. The obtained wavelet coefficients are analysed using various feature parameters available in literature with proposed fault indexing parameter (FIP). The FIP indicates the information about fault and its severity. This can be done using proposed ANN algorithm with various activation functions like tanh, sigmoid, ELU, and ReLU. Finally, the fault estimation of various faults using MCSA is obtained with 100% accuracy.

The rest of the paper is organized as the impact of various bearing faults and broken rotor faults which are discussed in Sect. 2, and mathematical analysis of proposed DWT-ANN is presented in Sect. 3. Section 4 presents the detailed topology

of fault detection using flow chart, and experimental evaluation is shown in Sect. 5. Finally, experimental results are discussed in Sect. 6.

2 Impact of Various Faults on MCSA

2.1 Bearing Faults

The roller and balls or rolling elements play a vital role in the rotational movement of rotor. Therefore, the roller element is treated as the crucial components of rotating electrical machines and immediate attention needs to be given for any type of abnormalities happening in ball bearing. Ball bearing typically consists of two rings: they are the way of outer race along with the inner raceway as per rolling balls set in their tracks. The rolling elements set or rolling balls located in races ways rotate inside these rings. Bearing problems [13–15] are occurred due to improperly forcing the bearing against the housing of bearing. This leads physical harm in brinelling form or maybe false brinelling of the raceways, which results in premature lack of bearing. These faults result in increased vibration, noise levels and temperature, and also cracking or bearings spalling will occur when small pieces cause by fatigue to break loose bearing. Faults in bearings can be caused by metal deformities, cracks and fragments on the surface raceway and can occur from a wide range of factors from contaminants in the raceways, improper installation, incorrect handling of the bearing, etc. The characteristic vibration frequencies due to inner race fault and outer race fault correspondingly "bearing pass frequency of inner race (BPFI)" and "bearing pass frequency of outer race (BPFO)" are computed with the following formulas [16, 17].

$$\mathrm{BPFI} = \frac{N_b f_r}{2}\left(1 + \frac{\mathrm{BD}}{\mathrm{PD}}\cos\phi\right) \tag{1}$$

$$\mathrm{BPFO} = \frac{N_b f_r}{2}\left(1 - \frac{\mathrm{BD}}{\mathrm{PD}}\cos\phi\right) \tag{2}$$

Here N_b represents the number of balls, f_r represents the speed of rotor in Hz, BD represents the diameter of ball bearing, PD represents the diameter of pitch, and ϕ represents the contact angle from the radial plane.

The stator current spectrum will reflect by changing the air gap flux density due to vibration frequencies of bearing defect. The stator current fault frequencies can be calculated from the fundamental component and vibration frequencies by using following equation.

$$f_\mathrm{bearing} = (f_s \pm m f_v) \tag{3}$$

where m = 1,2,3……, f_bearing is stator current fault frequency, f_s is supply frequency and f_v is vibration frequency of bearing faults.

2.2 Broken Rotor Faults

Generally, machines of low rating are made through the techniques of die casting and machines of huge ratings are made with copper rotor bar because the rotors are manufacturing by the die casting method, many technical problems can occur. The difficulties are due to technological impact, melting of end rings of rotor bars, many irregularities present in the squirrel cage induction motor. Conversely, in rotors failures may also have occurred due to several other reasons. These are.

- In manufacture during the process of brazing, metallurgical stresses, which are non-uniform, that might be occurred inside cage assembly along with these is main cause for the broken rotor bars.
- During the machine starting, a rotor bar might be unable to progress longitudinally in the period which inhabits the thermal stresses that are enforced on the rotor.
- Dangerous stresses on the bars can cause through heavy end ring which can result in heavy centrifugal forces.

Rotor bar might be injured; due to the above reasons, concurrent situation of unbalance rotor may take place. The rotor currents asymmetrical distribution is resulted due to rotor cage irregularity. Under the condition of broken rotor bars, the stator current components could be observed at given frequencies given by [18–21].

$$f_\mathrm{brb} = f_s\left[k\left(\frac{1-S}{P}\right) \pm S\right] \tag{4}$$

where f_brb = frequency of rotor bar. f_s = supply frequency. $k = 1,2,3\ldots p$ = pole pairs. s = per unit slip.

From Eq. (4), the fault frequencies due to broken rotor fault in a 3-phase induction motor can be obtained. It depends on the supply frequency, number of poles and speed of operation. As the speed changes due to load variations, the fault frequencies may vary. Moreover, the frequencies at any speed are side bands of fundamental component and the magnitude is varying depending on the fault severity.

3 Proposed Topology

3.1 Discrete Wavelet Transform

Fourier transform is utilized for signal processing during many years, because for the study of signals of a wide range it

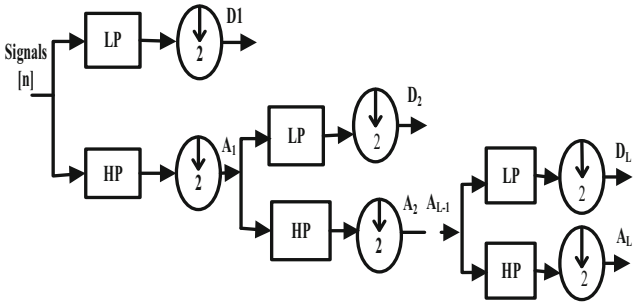

Fig. 1 Model of wavelet decomposition tree

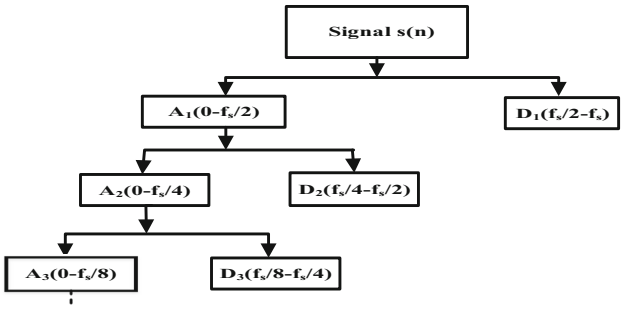

Fig. 2 Flow chart of frequency bands

is suitable. But merely the frequency content mining of signal is allowed in FFT, and also for the non-stationary signals analysis, it is not appropriate. To conquer this, short-term Fourier transform is utilized in the signal analysis in both frequency and time domain with the time window function but for data analysis concerning the optimum window size selection, some constraints are implied by it. To defeat these drawbacks, for analysing signals in frequency spectrum with varying time, the theory of wavelet is introduced. In discrete wavelet transform (DWT) [22–25], the signal is divided into two equal bandwidths with both high-pass and low-pass bandwidths. DWT at low-pass bandwidth gives high-frequency resolution, and at high-pass bandwidth it gives high time resolution. Using DWT, the decomposition of a sampled signal s(n) is performed into an approximation coefficient A_1 and detail coefficients D_1. Moreover, decomposition of A_1 produces two coefficients A_2 and D_2. Also decomposition of A_2 is shown in Fig. 1.

These decompositions are limited by number of levels that are obtained by

$$N_{\mathrm{LL}} = \mathrm{int}\left(\frac{\log \frac{f_s}{f_{su}}}{\log 2}\right) + 2 \tag{5}$$

where f_s represents sampling frequency and f_{su} represents fundamental frequency.

A discrete signal s(n) is decomposed as

$$s(n) = \sum_k a_{jo,k}\Phi_{jo,k}[n] + \sum_{j=j_o}^{j-1}\sum_k d_{j,k}\Phi_{j,k}[n] \tag{6}$$

where $\phi(n)$ represents scaling function of mother wavelet. $\Phi_{\mathrm{jo},k}[n]$ represent scaling function at scale $= 2^{jo}$ shifted by k. $\Phi_{j,k}[n]$ represent scaling function at scale $= 2^{ji}$ shifted by k. $a_{jo,k}$ represent approximation coefficient at scale 2^j. $d_{j,k}$ is a detail coefficient at scale 2^j.

As per the approach, which is presented in the research, the DWT application is proposed to the stator current. From the decomposition of DWT, approximation and detailed signals set is found. Within the original current signal, each one of the signals consists of time evolution of the components within its included corresponding frequency band. These signals analysis can allow some patterns detection caused by components evolution associated with bearing faults along with broken rotor bar faults. Daubechies-44 is employed for the analysis although other wavelet family also give satisfactory results. The decomposition tree of a signal with frequency bands is shown in Fig. 2.

3.2 Feature Extraction

Feature extraction is an important aspect for correct fault diagnosis, which is helpful in pattern recognition problems. An effective feature extraction gives the identification of abnormal conditions in the complete mathematical modelling of system or the analysis of fault current signatures resulting under different fault conditions. In the proposed circumstance, current signature analysis method is used for feature extraction. The stator current is decomposed into 8 levels by using Daubechies-44 mother wavelet; after decompositions, various features like energy, standard deviation, skewness, RMS and variance are calculated under healthy and faulty conditions of motor. Fault severity is estimated by comparing these features under healthy and faulty cases. Higher decomposition gives much clear fault identification comparing to lower decomposition levels.

The mathematical expressions for the corresponding time domain features are given below. where D_{k} (k = 1, 2… N) is amplitude of sampling point k and N is number of sampling points.

$$\text{Energy} = \sum_{k=1}^{N} (D_k)^2 \tag{7}$$

$$\text{Standard deviation (SD)} = \sqrt{\frac{1}{N}\sum_{K=1}^{N}\left(D_k - \overline{D}_k\right)}^2 \tag{8}$$

$$\text{Skewness (SK)} = \frac{\frac{1}{N}\sum_{k=1}^{N}\left(D_k - \overline{D}_k\right)^3}{(SD)^3} \tag{9}$$

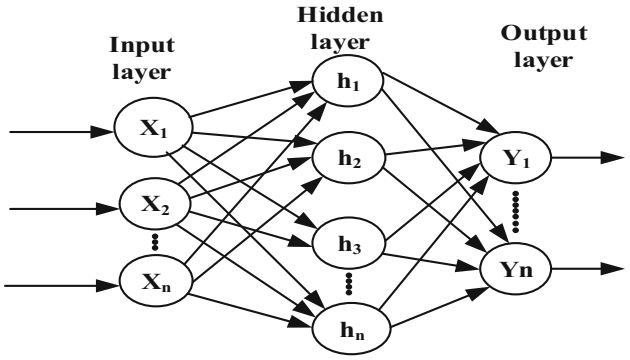

Fig. 3 Architecture of neural network

$$\text{Root mean square value (RMS)} = \sqrt{\frac{1}{N}\sum_{k=1}^{N}(D_k)^2} \quad (10)$$

$$\text{Variance (VAR)} = \frac{1}{N}\sum_{k=1}^{N}\left(D_k - \overline{D}\right)^2 \quad (11)$$

3.3 Artificial Neural Network

Neural network classifier is the most used deep learning classifiers which consist of the various interconnected processing unit called neurons. Each neuron is associated with an activation function which is simple differential function of mathematics. General structure of neural network contains three types of layers, namely hidden layer, input layer and output layer. Every layer is formed by multiple neurons that are interconnected to each other's. Number of input and output present in the recognizing pattern determines the neurons number required in network structure's input and output layers. Number of hidden layers and its neurons governs the learning capability of neural network [26] Input layer takes the features as input, and these features are passed to different layers of hidden layer and then passed to output layer. Each layer's neuron is characterized by weight value. By making suitable architecture and modifying these weights according to some rules, to identify any pattern neural network can be trained. Accuracy is directly depending on the type of problem, which used neural network architecture and hyperparameter tuning. Various types of neural network architecture are there; for the diagnosis purposes among them, the multilayer perceptron is most popular one which is adopted in the present study. Neural network's general structure is represented in Fig. 3.

If model architecture has n layers and h hidden neurons in each layer, then one-output neurons can be expressed as

$$Y = G_k \sum_{h=1}^{H} O_h Y_h W_h W_o \quad (12)$$

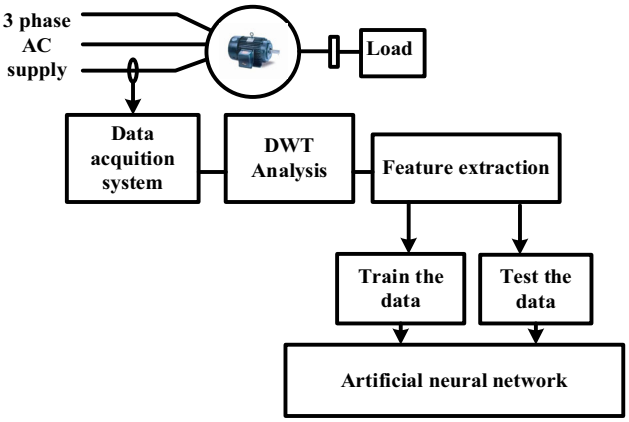

Fig. 4 Block diagram of proposed methodology of fault diagnosis in IM

where$Y$ is the output.G_{k} represents the activation function.O_{h} represents an output value of the hth hidden neurons, being O_{h} given as

$$O_h = G_k \sum_{h=1}^{H} X_n W_{nh} W_{oh} \quad (13)$$

whereX_{n} are the MLP input. $G_{\mathrm{k}}$is the activation function. W_{oh} and W_{nh} are the synaptic weights between the hidden.

Neurons, MLP outputs and input, respectively.

4 Proposed Scheme of Fault Detection using DWT-ANN

In this section, proposed scheme of fault detection is presented and has 5 stages of signal processing. The block diagram representation of proposed methodology of DWT-ANN algorithm for the fault diagnosis of bearing and broken rotor bar faults is represented in Fig. 4. The flow chart for the proposed algorithm is mentioned in Fig. 5.

In the first stage, the stator current under faulty as well as healthy circumstances is acquired by current sensor and data acquisition system. The data collection is done using national instrument (NI) make myDAQ in the Lab VIEW environment. The stator current is acquired at 10 kHz sampling rate under different load conditions. The specifications of test motor, faults considered for examination of proposed work and various load condition are presented in Sect. 5.

In the next stage, DWT analysis is carried out for acquired signals from the motor. In this, stator current is decomposed into approximation and detail coefficients using DWT analysis based on speed range, sampling frequency, etc. The DWT decomposition is done at 8 levels for good resolution and as well as minimum mathematical computations as discussed in Sect. 6. In this level of decomposition, 8 detailed coefficients and 1 approximated coefficient are available for analysis.

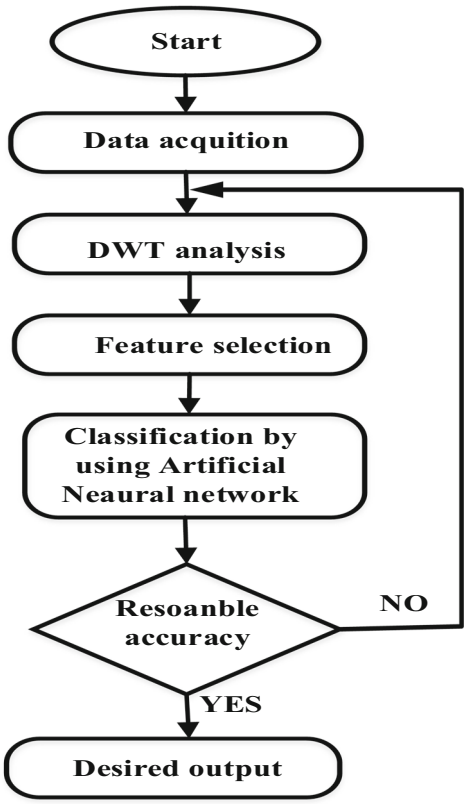

Fig. 5 Flow graph of proposed fault detection algorithm using DWT based ANN

Due to a greater number of coefficients available at this stage, feature computation is proposed and carried out in the next stage.

Various features, namely energy, standard deviation (SD), skewness, RMS value, and variance, are proposed in this work. The mathematical expressions are discussed from Eqs. (7) to (11) in the previous section. These parameters are used to analyse the obtained wavelet coefficients at different conditions of the motor. Then proposed fault indexing parameter (FIP) is analysed to evaluate the seriousness of the fault. The FIP is computed by taking the ratio of faulty features to healthy features. As this is 1 under healthy condition of the motor, the fault severity is estimated based on the increment of FIP from 1. The manual comparison of this process leads to wrong diagnosis and time delay; ANN-based algorithm is proposed in the next stage.

In this stage, the fault accuracy is calculated by using artificial neural networks with different activation functions like tanh, sigmoid, ELU, and ReLU. The detailed mathematical analysis is presented in the previous section. In this, tanh activation function gives best accuracy compared to other proposed functions. The detailed performance of these functions is discussed in results section.

Finally, decision algorithm is performed as shown in the flowchart in Fig. 5. If the accuracy is less than 100%, the total procedure is repeated, or else fault is announced.

5 Experimental Set-up

An experimental set-up was specially designed for acquiring current signal from the motor under various fault conditions as illustrated in Fig. 6. The set-up consists of a 1. 5-Kw 3-phase squirrel cage induction motor, motor loading arrangement along with NIMYDAQ data acquisition system associated to the laptop. Under full load conditions, one acquires the data from the motor running from the following conditions which are given as:

1. Healthy motor
2. Inner race defect of bearing (BIRF)
3. Outer race defect of bearing (BORF)
4. Broken rotor bars (3-BRB)

Bearing defects were formed by creating holes (5mm diameter) on the outer and inner races of ball bearings as shown in Fig. 6. Initially from the motor, the current data acquired in healthy conditions and subsequent current data are acquired with inner race defect and outer race defect faulty bearings. On the rotor by drilling 6-mm-diameter holes, broken rotor bar faults were created, so as a result the bar is fully isolated. From motor, the present signal was obtained with 3 broken rotor bars. The current signal is obtained from motor utilizing an NI MYDAQ data acquisition system and current sensor.

6 Results and Discussion

In given section bearing fault diagnosis, broken rotor bars experimental result in 3-phase induction motor was explained. In Fig. 4, the proposed topology block diagram is displayed. Initially from the data acquisition system, the stator current is acquired under healthy and various fault conditions. Afterwards, utilizing wavelet analysis stator current is decomposed in approximated as well as detail coefficients. The various feature parameters, such as energy (E), standard deviation (SD), skewness (SK), RMS value (RMS), and variance (VAR) of corresponding wavelet coefficients, are calculated and used as fault indexing parameters. Fault severity is expected compelling the ratio of faulty signal feature value to the healthy signal feature value. Under good condition of motor fault, indexing parameter (FIP) should be 1. As the fault severity increases, FIP increases correspondingly. In last stage, fault detection accuracy can be determined by

Fig. 6 Bearings with healthy, inner race defect, outer race defect and rotor with 3 hole (3-BRB)

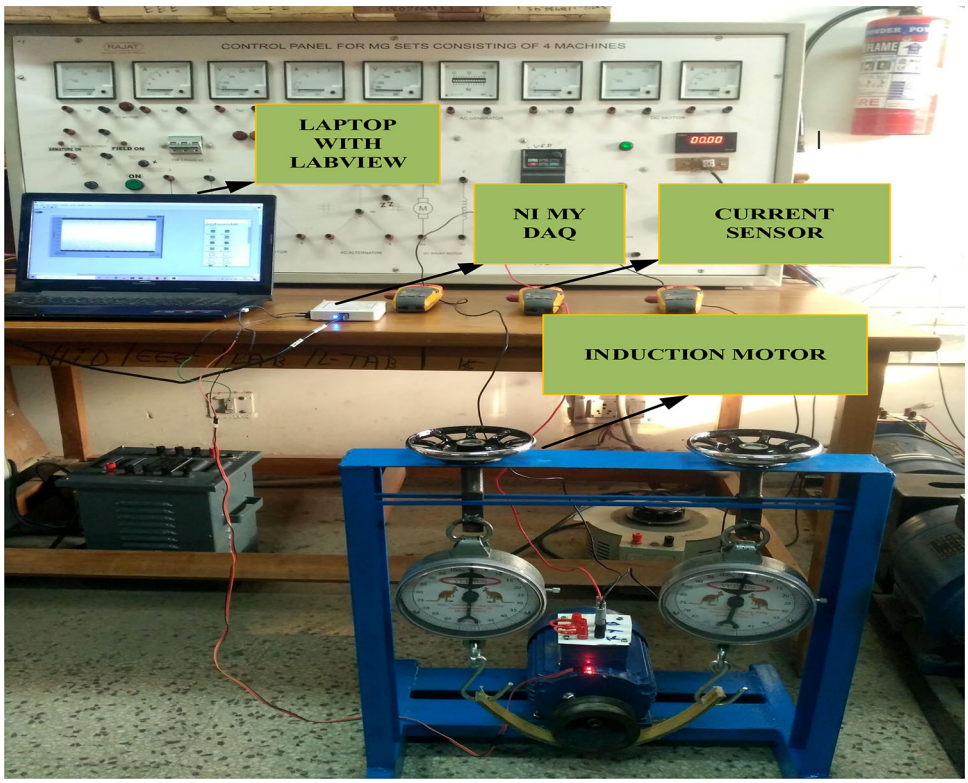

Fig. 7 Experimental Setup

Table 1 Specifications of ball bearings

Specification	Values
Bearing no	6205-ZZ
Type	Deep grooved ball bearing
Contact angle	0 degrees
Ball diameter (BD)	3. 89 mm
Pitch diameter(PD)	7. 92 mm
Number of balls	9

Table 2 Machine details

Name plate details	Rating
Power	1.5 kw
Speed	1415–1500 rpm
Voltage	440
Current	3.2 A

using artificial neural network model with different activation functions (Tables 1, 2, 3, 4).

6.1 DWT Analysis

In given section, wavelet analysis of stator current is achieved by Daubechies's wavelet function of family 44 (db44) along with approximation and detail coefficients are calculated of healthy and faulty signals. As the DWT has huge number of coefficients at higher-level decomposition, which is essential

Table 3 Bearing fault frequencies

	No load frequencies(Hz)		Full loadfrequencies(8. 67N–M) (Hz)	
	f_{in}	f_{out}	f_{in}	f_{out}
f_r	24.7	24.7	23.8	23.8
$m = 1$	215.7	106.5	209.7	104.5
$m = 2$	381.4	163.1	369.4	158.9
$m = -1$	105.7	6.5	109.7	4.5
$m = -2$	281.4	63.1	269.4	58.9

Table 4 Broken rotor fault frequencies

	No load frequencies(Hz)		Full loadfrequencies(8. 67 N-M) (Hz)	
	Left-side band frequencies	Right-side band frequencies	Left-side band frequencies	Right-side band frequencies
K = 1	49	51	45.3	54.7
K = 2	48	52	40.6	59.3

LSB-Left-side band frequencies; RSB-right-side band frequencies

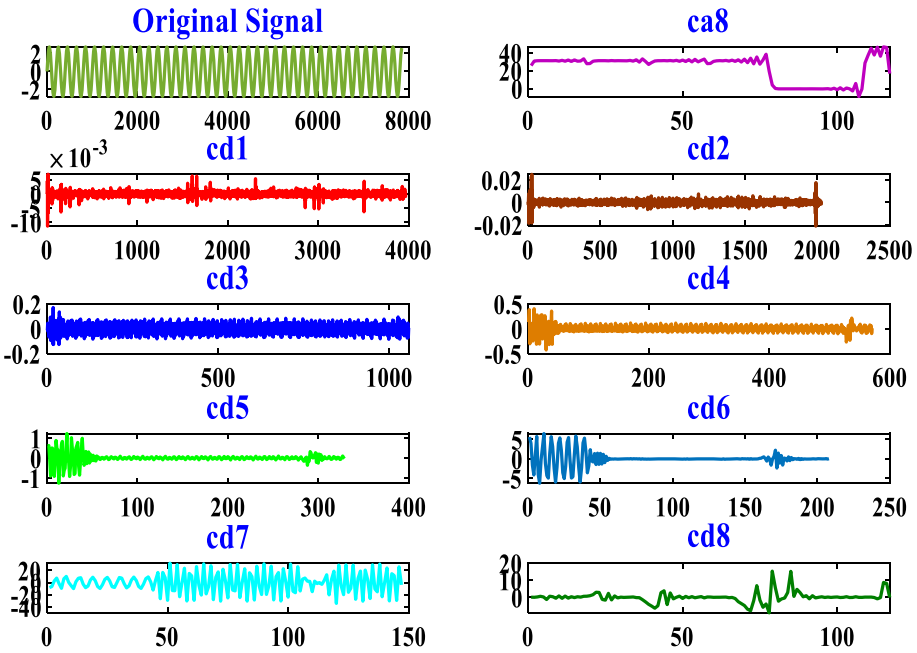

Fig. 8 Wavelet decomposition of healthy stator current signal

for good resolution, analysis of wavelet coefficients becomes difficult and leads to wrong diagnosis of the machine. Further it requires more mathematical calculations and leads to delay in fault detection. Therefore, DWT along with various features energy, standard deviation, skewness, RMS value and variances is used for fault diagnosis. In continuation to this, fault indexing parameter is calculated to estimate the severity of the fault. The fault indexing parameter is defined as the ratio of feature parameter of fault signal to feature parameter of healthy signal. Under normal condition of the machine, this FIP is equal to 1 and increases when fault occurs. The decompositions of healthy stator current and bearing, broken rotor bar fault stator current of are shown in Figs. (8, 9, 10, 11). The feature values of healthy signal and different faults signals are tabulated corresponding as given in Tables 5,6,7,8.

From Figs. (12, 13, 14, 15, 16), it is understanding that under healthy condition of motor, corresponding energy, standard deviation, skewness, RMS, variance values are less compared to different fault conditions. Fault severity can be estimated by comparing the ratio of these parameters under healthy and faulty conditions. It is clearly observed that compared to the lower decomposition levels, the higher

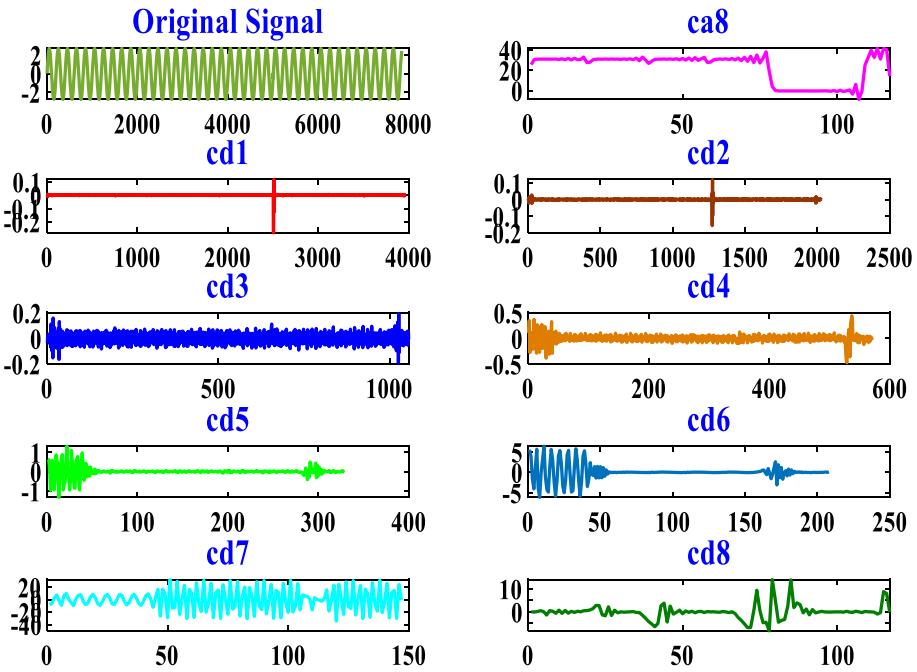

Fig. 9 Wavelet decomposition of BIRF stator current signal

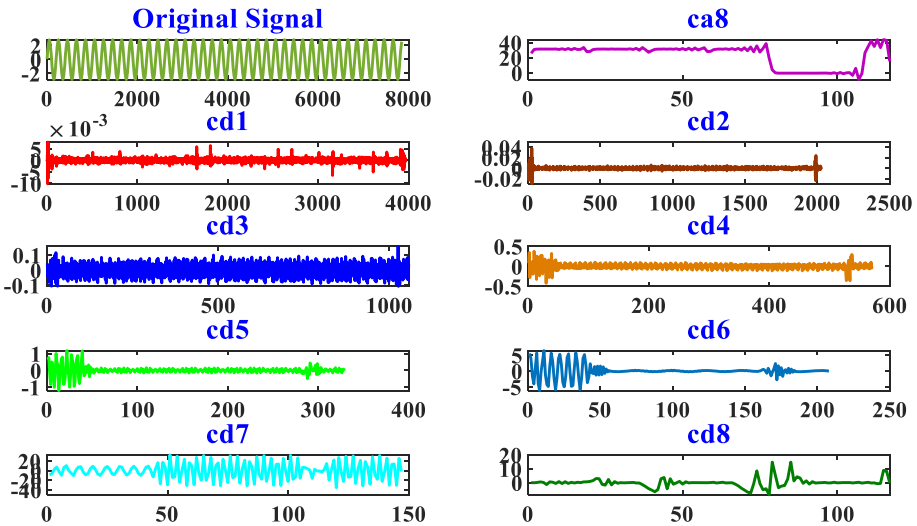

Fig. 10 Wavelet decomposition of BORF stator current signal

decomposition level gives much clear fault identification. If the decomposition level is low, very few wavelet coefficients are available for analysis and difficult to estimate the nature of fault. In low-level decomposition, length of the coefficients is also high and hence resolution is poor. In contrast to this, if the decomposition level is high, a greater number of wavelet coefficients are available and resolution is very good. But mathematical analysis becomes difficult and leads to non-reliable diagnosis of the motor. Therefore, level of decomposition is neither too low nor too high. To overcome this problem, selection of decomposition level also plays a vital role in fault identification. Moreover, direct analysis of wavelet coefficients does not give any information about fault, and hence, features are computed for wavelet coefficients. The plots of energy, standard deviation and variance show much clear fault identification and compare to other features under healthy and faulty condition of motor. The plots of RMS and skewness are narrow separation between healthy and faulty cases, which give less identification. These features set used to train ANN model. Fault detection accuracy is determined by means of a six-layer neural network with different activation functions.

6.2 Accuracy Performance by ANN Model

Multilayer perceptron (MLP) required updating the weight values on each iteration, to minimize the output error. This

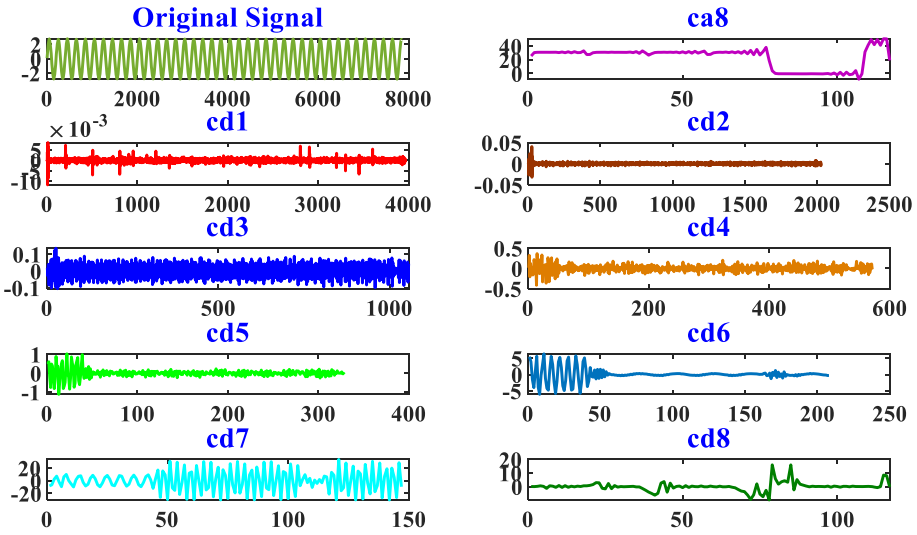

Fig. 11 Wavelet decomposition of 3-BRB stator current signal

Table 5 Fault indexing parameters (FIPS) of healthy stator current signal

Wavelet levels	Healthy stator current signal				
	Energy(E)	Standard deviation(SD)	RMS value	Skewness	Variance
D1	0.96	1.01	0.98	0.20	1.00
D2	1.02	1.21	1.02	0.26	1.02
D3	1.04	1.23	1.22	0.31	1.02
D4	1.12	1.26	1.25	0.33	0.98
D5	1.31	1.27	1.27	0.36	1.03
D6	1.41	1.29	1.29	0.37	1.03
D7	2.01	1.33	1.32	0.37	1.04
D8	3.32	1.38	1.37	0.38	1.04

Table 6 Fault indexing parameters (FIPS) of inner race fault stator current signal

Wavelet levels	Inner race fault stator current signal				
	Energy(E)	Standard deviation(SD)	RMS value	Skewness	Variance
D1	1.61	1.32	1.51	0.23	1.01
D2	1.63	1.64	1.49	0.27	1.02
D3	1.67	1.78	1.49	0.35	1.02
D4	1.72	1.79	1.45	0.38	0.99
D5	1.96	1.82	1.43	0.37	1.11
D6	2.92	1.93	1.36	0.41	1.46
D7	3.29	2.52	1.37	0.45	1.48
D8	5.56	4.56	1.52	0.48	1.52

process is done by back propagation learning algorithm. This algorithm mainly computes the error of training cases and recursively change the network weight and biases such that error gets minimized. This process is repeated until the error reduces or reached the defined goal. Due to high pattern recognition capability and complex mapping ability, an ANN could be efficiently utilized in fault classification of induction motor. To implement ANN model, the entire feature, which was obtained by data pre-processing and DWT analysis, is send to input layer of ANN. For generalization, MLP should be trained on different architecture and different combination of hyperparameter, which is mentioned in Tables 9, 10. For all considered combination of hyperparameter, total data are divided into training data (50%) and testing data (50%), with step size of 0. 1 and momentum of 0. 9. Each output layer contains the five SoftMax processing unit, and each

Table 7 Fault indexing parameters (FIPS) of outer race fault stator current signal

Wavelet levels	Outer race fault stator current signal				
	Energy(E)	Standard deviation(SD)	RMS value	Skewness	Variance
D1	1.67	1.34	1.52	0.25	1.03
D2	1.82	1.71	1.48	0.28	1.11
D3	1.94	1.82	1.49	0.36	1.13
D4	2.01	1.93	1.46	0.38	1.18
D5	2.21	2.01	1.38	0.39	1.21
D6	2.32	2.32	1.39	0.43	1.49
D7	3.65	2.78	1.52	0.51	1.57
D8	5.84	4.87	1.58	0.53	1.68

Table 8 Fault indexing parameters (FIPS) of 3-BRB fault stator current signal

Wavelet levels	3-BRB fault stator current signal				
	Energy(E)	Standard deviation(SD)	RMS value	Skewness	Variance
D1	2.21	1.38	1.53	0.26	1.05
D2	2.32	1.78	1.49	0.29	1.13
D3	2.37	2.31	1.48	0.39	1.15
D4	2.38	2.53	1.46	0.39	1.19
D5	2.81	2.91	1.39	0.40	1.26
D6	3.52	3.32	1.37	0.48	1.52
D7	4.23	3.91	1.41	0.55	1.63
D8	6.42	5.23	1.42	0.61	1.73

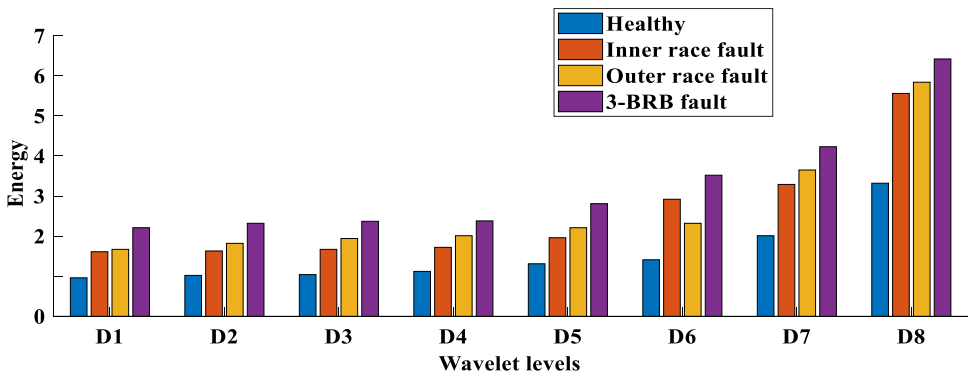

Fig. 12 Bar graph of energy under healthy and different fault conditions

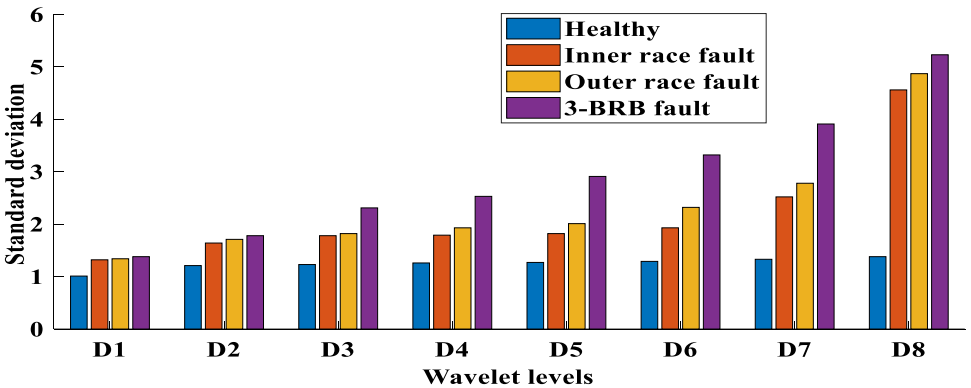

Fig. 13 Bar graph of energy under healthy and different fault conditions

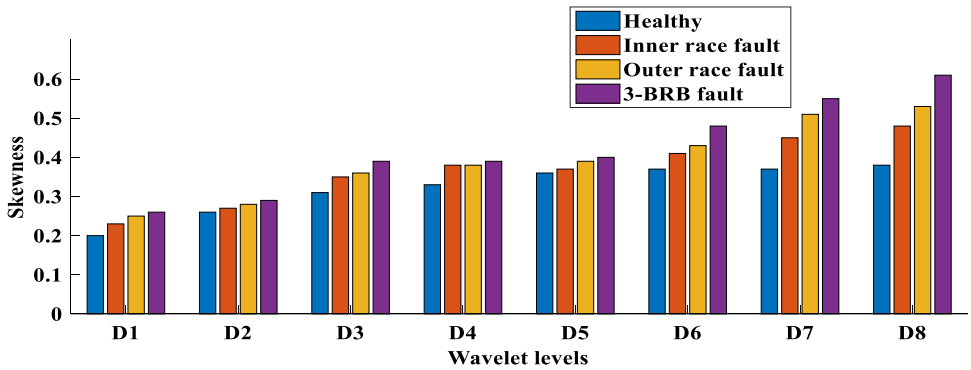

Fig. 14 Bar graph of skewness under healthy and different fault conditions

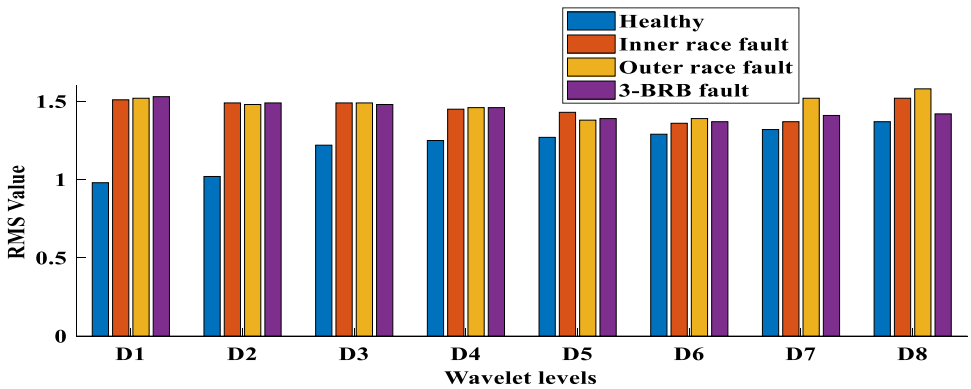

Fig. 15 Bar graph of RMS value under healthy and different fault conditions

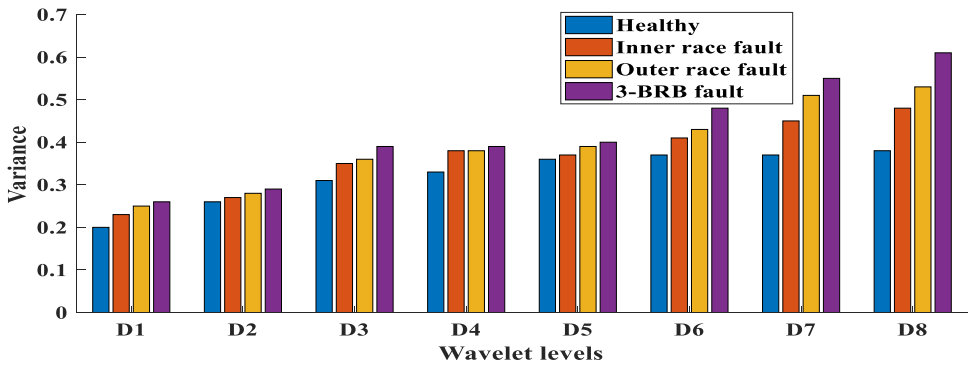

Fig. 16 Bar graph of variance under healthy and different fault conditions

Table 9 Set of combinations taken to analyse the model

Hyper parameter	Range of hyper parameter
Activation function	Tanh, sigmoid, ELU, ReLU
Number of neurons in a layer	16, 32, 64, 128, 256
Hidden layers	1, 2, 3, 4, 5, 6
Batch size	5–20
No of epochs	8, 16, 32, 64, 128, 256
Dropout rate	10–30%

Table 10 Comparisons of various functions of ANN model

Parameters	Tanh	Sigmoid	ELU	ReLU
No of hidden layers	4	5	6	3
No of nodes	64	256	128	128
Dropout (%)	10	20	5	10
Epochs	128	256	256	256
Batch Size	5	5	10	10
Test accuracy	100	86	100	100
Test loss	9.8 e-5	0.6678	0.0125	0.0065

model is optimized on the Adam optimizer and categorical cross-entropy loss function.

The plot of Fig. 17A–D represents classification accuracy of comparative analysis with respect to various activation functions mentioned in Table 11. In each combination, Soft-Max function is used as activation function of output layer to normalize the output into probability distribution. This paper

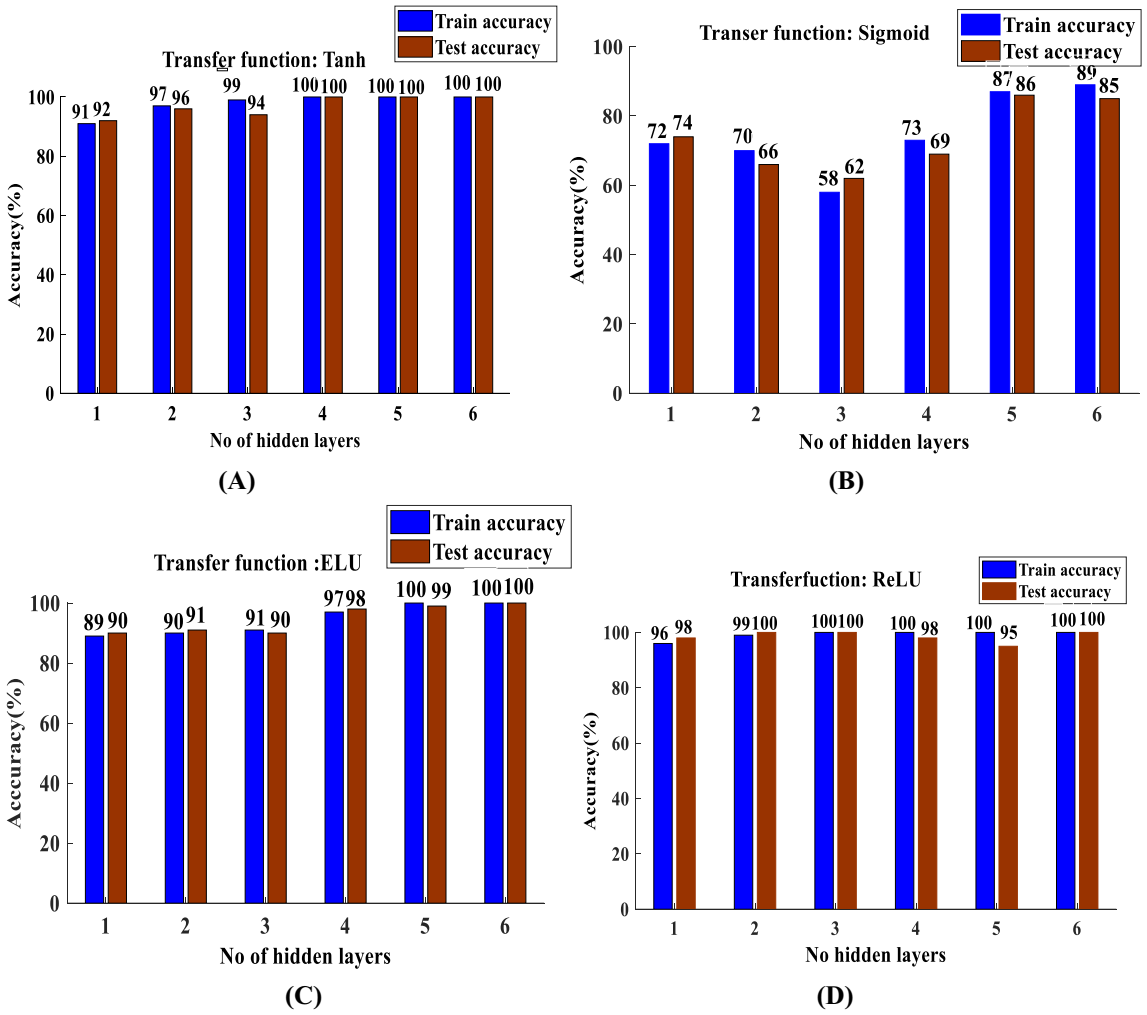

Fig. 17 Training and testing accuracy of different functions: **A** tanh, **B** sigmoid, **C** ELU and **D** ReLU

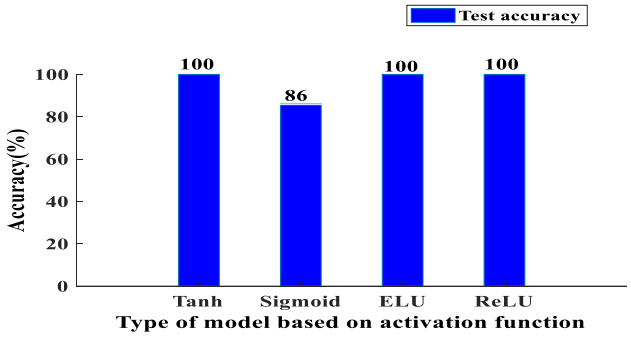

Fig. 18 Best accuracy of each optimized model

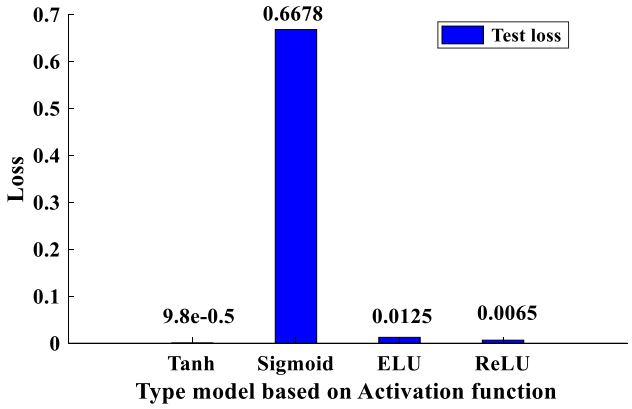

Fig. 19 Loss of each optimized model

used grid search algorithm to find out the best hyperparameter corresponding to each activation function. Figure 17A shows the variation of train and test accuracy of tanh activation function with respect to numeral of hidden layer processing by taking the best no of neurons in each layer, best percentage of dropout, best no of epoch and batch size that are obtained by grid search keeping activation function and hidden layer fixed at a time. Figure 17B shows the variation of train and test accuracy of sigmoid function with respect to numeral of hidden layer processing by taking the best no

Table 11 Comparisons of various functions of ANN model

Number of hidden layers	Training accuracy (%)				Testing accuracy(%)			
	Tanh	Sigmoid	ELU	ReLU	Tanh	Sigmoid	ELU	ReLU
1	91	72	89	96	92	74	90	98
2	97	70	90	99	96	66	91	100
3	99	58	91	100	94	62	90	100
4	100	73	97	100	100	69	98	98
5	100	87	100	100	100	86	99	95
6	100	89	100	100	100	85	100	100

of neurons in each layer, best percentage of dropout, best no of epoch and batch size that are obtained by grid search keeping activation function and hidden layer fixed at a time. Figure 17C shows the variation of train and test accuracy of ELU function with respect to numeral hidden layer processing by taking the best no of neurons in each layer, best percentage of dropout, best no of epoch and batch size that are obtained by grid search keeping activation function and hidden layer fixed at a time Fig. 17D shows the variation of train and test precision of ReLU function with respect to numeral of hidden layer processing by taking the best no of neurons in each layer, best percentage of dropout, best no of epoch and batch size that are obtained by grid search keeping activation function and hidden layer fixed at a time.

After implementing and optimizing various model of ANN, it is found that the model contains the tanh activation function which performs very well in comparison with other activation functions. To analyse the best model out of four optimized model of different activation functions, plot of test accuracy and test loss of each best four models are shown in Figs. (18, 19). Loss of tanh function is lesser than other models, and accuracy is more than others; it gives 100% accuracy. So finally, it is found that model which is obtained by the grid search algorithm on the tanh activation function gives the best classification result and easily can be used to diagnosis of faults in Induction motor.

The results obtained using proposed work are evaluated by comparing with existed work in the literature. The accuracy of the proposed DWT-ANN with activating function of tanh is compared with various algorithms and plotted in Fig. 20, and the same is also presented in table format in Table 12.

7 Conclusion

This paper presents an accurate fault diagnosis as well as faults classification in induction motor which depends on discreet wavelet transform and artificial neural networks (DWT-ANN). The mother wavelet Daubechies-44 with 8 decomposition levels is used for wavelet decomposition. After wavelet decomposition of stator current, various features like energy, standard deviation, skewness, RMS and variance are determined under healthy and faulty conditions of the motor. Fault severity is estimated by compelling the ratio of faulty feature values to healthy feature values. The fault severity estimation is good at minimum of 8 levels compared to other decomposition level. The fault classification is done using ANN with various functions, and tanh function gives very good accuracy compared to other functions like sigmoid, ReLU and ELU. The proposed method using the grid search algorithm to find the best combination of hyperparameter which try the all the combination of parameter and return them which corresponding the most accuracy. The accuracy of the proposed work is 100% and is more compared to other popular algorithms ELM, KNN, SVM, NBC and ANN with WPD. Along with accuracy, other classification performance evaluating parameter like precision, recall and F1 score is also 100%. So, DWT-ANN-based classifier can easily use to solve the problem of accurate fault diagnosis of induction motor. In future, various other faults like stator interturn, eccentricity and various bearing faults can be tested.

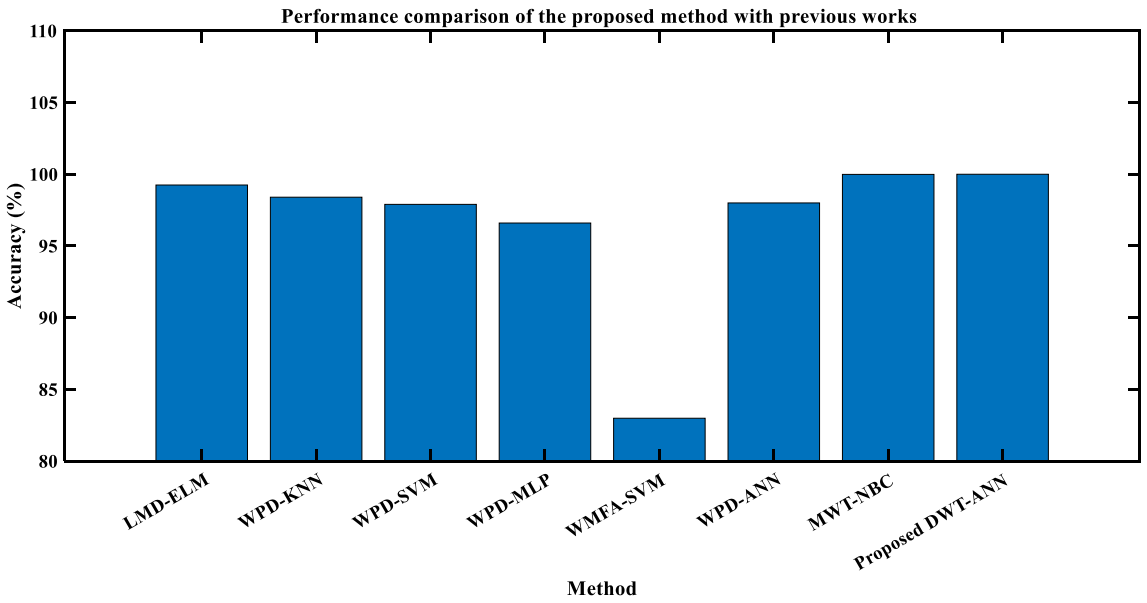

Fig. 20 Comparison of proposed work with existed literature

Table 12 Performance comparison the proposed method with previous works

Ref	Feature extraction	Number of features	Fault types	Classifier	Test loss	Classification accuracy (%)
[25]	LMD-SVD	40	BF, BIRF, BORF	ELM	NA*	ELM 99.25
[26]	Envelope analysis and wavelet packet analysis	130	BF, BIRF, BORF	kNN, SVM, and MLP	NA*	kNN 98.4; SVM 97.9; MLP 96.6
[27]	Wavelet multi fractal analysis	25	BF, BIRF, BORF	SVM	NA*	SVM 82.99
[28]	WPD	2	BRB1,BRB 2	ANN	NA*	ANN 98
[17]	MWT	18	BF, BIRF, BORF	NBC	NA*	NBC 99.99
Proposed method	DWT	5	BIRF,BORF, BRB 3	ANN	9. 8e-5	ANN100

**NA* not available; *BIRF* inner race fault; *BF* ball fault; *BORF* outer race fault; *BRB* broken rotor fault; *NBC* naive Bayes classifier; *kNN* k-nearest neighbour; *SVM* support vector machine; *MLP* multilayer perceptron; *ANN* artificial neural network; *DWT* discrete wavelet transforms; *MWT* multiwavelet transform; *WPD* wavelet packet decomposition; *LMD-SVD* local mean decomposition-singular value decomposition; *ELM* extreme learning machine

References

1. Patel, R.A.; Bhalja, B.R.: Condition monitoring and fault diagnosis of induction motor using support vector machine. Electr Power Compon Syst **44**(6), 683–692 (2016). https://doi.org/10.1080/15325008.2015.1131762
2. Yang, S.K.: A condition-based failure-prediction and processing-scheme for preventive maintenance. IEEE Trans. Reliab. **52**(3), 373–383 (2003). https://doi.org/10.1109/TR.2003.816402
3. Dahi K, Elhani S, Guedira S, Sadiki L, Ouachtouk I (2015) High-resolution spectral analysis method to identify rotor faults in WRIM using Neutral Voltage. https://doi.org/10.1109/EITech.2015.7162988
4. Wang, X.; Fang, F.: Bearing failure diagnosis in three-phase induction motor by chirp-Z transform and Zoom-MUSIC. Int Conf Electr Control Eng ICECE (2011). https://doi.org/10.1109/ICECENG.2011.6057197
5. Cocconcelli, M.; Zimroz, R.; Rubini, R.; Bartelmus, W.: STFT based approach for ball bearing fault detection in a varying speed motor. In: Condition monitoring of machinery in non-stationary operations. Springer, Berlin, Heidelberg (2012)
6. Rosero, J.; Romeral, L.; Ortega, J.A.; Rosero, E.: Short circuit fault detection in PMSM by means of empirical mode decomposition (EMD) and wigner ville distribution (WVD). Conf Proc IEEE Appl Power Electron Conf Expos APEC (2008). https://doi.org/10.1109/APEC.2008.4522706
7. Konar, P.; Chattopadhyay, P.: Bearing fault detection of induction motor using wavelet and Support Vector Machines (SVMs). Appl Soft Comput J (2011). https://doi.org/10.1016/j.asoc.2011.03.014

8. Kompella, K.C.D.; Mannam, V.G.R.; Rayapudi, S.R.: DWT based bearing fault detection in induction motor using noise cancellation. J Electr Syst Inf Technol (2016). https://doi.org/10.1016/j.jesit.2016.07.002
9. Kompella, K.C.D.; Rao, M.V.G.; Rao, R.S.: SWT based bearing fault detection using frequency spectral subtraction of stator current with and without an adaptive filter. IEEE Region Annu Int Conf Proc TENCON 2017 (2017). https://doi.org/10.1109/TENCON.2017.8228277
10. Samanta, B.; Al-Balushi, K.R.: Artificial neural network based fault diagnostics of rolling element bearings using time-domain features. Mech Syst Signal Process (2003). https://doi.org/10.1006/mssp.2001.1462
11. Agrawal, P.; Jayaswal, P.: Diagnosis and classifications of bearing faults using artificial neural network and support vector machine. J Inst Eng Series C (2020). https://doi.org/10.1007/s40032-019-00519-9
12. Kumar, R.S., et al.: A method for broken bar fault diagnosis in three phase induction motor drive system using Artificial Neural Networks. Int J Ambient Energy (2021). https://doi.org/10.1080/01430750.1934117
13. Rai, A.; Upadhyay, S.H.: A review on signal processing techniques utilized in the fault diagnosis of rolling element bearings. Tribol Int (2016). https://doi.org/10.1016/j.triboint.2015.12.037
14. Singh, S.; Kumar, A.; Kumar, N.: Motor current signature analysis for bearing fault detection in mechanical systems. Procedia Materials Science (2014). https://doi.org/10.1016/j.mspro.2014.07.021
15. Toma, R.N.; Prosvirin, A.E.; Kim, J.M.: Bearing fault diagnosis of induction motors using a genetic algorithm and machine learning classifiers. Sensors (2020). https://doi.org/10.3390/s20071884
16. Trajin, B.; Regnier, J.; Faucher, J.: Comparison between vibration and stator current analysis for the detection of bearing faults in asynchronous drives. IET Electr Power Appl (2010). https://doi.org/10.1049/iet-epa.2009.0040
17. Saini, M.K.; Aggarwal, A.: Detection and diagnosis of induction motor bearing faults using multiwavelet transform and naive Bayes classifier. Int Trans Electr Energy Syst (2018). https://doi.org/10.1002/etep.2577
18. Zaman, S.M.K.; Marma, H.U.M.; Liang, X.: Broken rotor bar fault diagnosis for induction motors using power spectral density and complex continuous wavelet transform methods. IEEE Canadian Conf Electr Comput Eng CCECE 2019 (2019). https://doi.org/10.1109/CCECE.2019.8861517
19. Hassan, O.E.; Amer, M.; Abdelsalam, A.K.; Williams, B.W.: Induction motor broken rotor bar fault detection techniques based on fault signature analysis—a review. IET Electr Power Appl (2018). https://doi.org/10.1049/iet-epa.2018.0054
20. Chahine, K.: Rotor fault diagnosis in induction motors by the matrix pencil method and support vector machine. Int Trans Electr Energy Syst (2018). https://doi.org/10.1002/etep.2612
21. Ramu, S.K.; Raj Irudayaraj, G.C.; Subramani, S.; Subramaniam, U.: Broken rotor bar fault detection using Hilbert transform and neural networks applied to direct torque control of induction motor drive. IET Power Electron (2020). https://doi.org/10.1049/iet-pel.2019.154
22. Ali, M.Z.; Liang, X.: Induction motor fault diagnosis using discrete wavelet transform. 2019 IEEE Can Conf Electr Comput Eng (2019). https://doi.org/10.1109/CCECE.2019.8861923
23. Defdaf, M.; Berrabah, F.; Chebabhi, A.; Cherif, B.D.E.: A new transform discrete wavelet technique based on artificial neural network for induction motor broken rotor bar faults diagnosis. Int Trans Electr Energy Syst (2021). https://doi.org/10.1002/2050-7038.12807
24. Ali, M.Z.; Liang, X.: Induction motor fault diagnosis using discrete wavelet transform. 2019 IEEE Canadian Conf Electr Comput Eng (2019). https://doi.org/10.1109/CCECE.2019.8861923
25. Tian, Y.; Ma, J.; Lu, C.; Wang, Z.: Rolling bearing fault diagnosis under variable conditions using LMD-SVD and extreme learning machine. Mech Mach Theory (2015). https://doi.org/10.1016/j.mechmachtheory.2015
26. Rauber, T.W.; de Assis Boldt, F.; Varejão, F.M.: Heterogeneous feature models and feature selection applied to bearing fault diagnosis. IEEE Trans Ind Electr (2014). https://doi.org/10.1109/tie.2014.2327589
27. Du, W.; Tao, J.; Li, Y.; Liu, C.: Wavelet leaders multifractal features based fault diagnosis of rotating mechanism. Mech Syst Signal Process (2014). https://doi.org/10.1016/j.ymssp.2013.09.003
28. Sadeghian, A.; Ye, Z.; Wu, B.: Online detection of broken rotor bars in induction motors by wavelet packet decomposition and artificial neural networks. IEEE Trans Instrum Measure (2009). https://doi.org/10.1109/tim.2009.2013743